THE IMPORTANCE OF FLUCTUATIONS*

Gösta Gustafson

Department of Theoretical Physics, Lund University
Sölveg. 14A, 22362 Lund, Sweden
gosta.gustafson@thep.lu.se

(Received November 11, 2011)

Dedicated to Andrzej Białas in honour of his 75th birthday

In this contribution I want to discuss three phenomena, where effects of fluctuations are very important, multiplicity distributions, diffractive excitation, and nucleus collisions.

DOI:10.5506/APhysPolB.42.2571
PACS numbers: 12.38.–t, 13.60.Hb, 13.85.–t

1. Introduction

In Andrzej Białas' scientific production fluctuations are a very common theme. Some examples are studies of multiplicity distributions, intermittency, BE correlations, and saturation effects in the BK equation. Fluctuations are also an important ingredient in many analyses by the Lund group, and in this talk I want to discuss a few of them: First some early results on *Multiplicity Distributions*, then recent results on *Diffraction*, and finally, studies of *Nucleus Collisions*, which will be ready soon.

2. Multiplicity distributions

In e^+e^- annihilation the process contains two phases, an initial perturbative phase described as a gluon cascade, followed by a nonperturbative phase, where the energy of the partons is transformed into hadrons. The Lund dipole cascade model is illustrated in Fig. 1 (left), which shows the phase space for gluon emission in a rapidity (horizontal) — $\ln k_\perp^2$ (vertical) plot. This figure has a fractal structure with large fluctuations [1]. The

* Presented at the LI Cracow School of Theoretical Physics "Soft Side of the LHC", Zakopane, Poland, June 11–19, 2011.

hadronization in the Lund string model has smaller fluctuations of a Poissonian nature. The fluctuations in the two subprocesses are shown in Fig. 1 (right), together with the result obtained for the total process [2]. We note here that although none of the two subprocesses is scaling by itself, the combined result exhibits almost perfect scaling, with the variance proportional to the square of the average multiplicity. For very high energy, the fluctuations in the cascade dominate, which approaches scaling asymptotically, but for energies in the PETRA–LEP range this feature appears to be more of a coincidence.

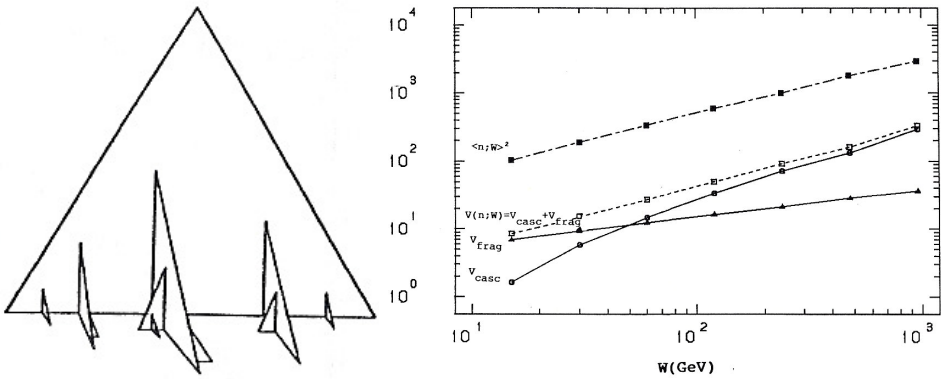


Fig. 1. Left: The phase space for gluon emission in e^+e^- annihilation in a $(y-\ln k_\perp^2)$ diagram. Right: The contributions to the variance of the multiplicity distribution from the parton cascade and from the soft fragmentation. The total result (dash–dotted) is scaling and proportional to the squared average (dotted).

3. Diffractive excitation

3.1. Good–Walker formalism

Diffraction and saturation are most easily described in impact parameter space, within the eikonal approximation. If the interaction is driven by absorption into inelastic states i, with weights $2f_i$, the optical theorem gives an elastic amplitude given by

$$T = 1 - e^{-F}\,, \quad \text{with} \quad F = \sum f_i\,. \tag{1}$$

For a structureless projectile we then find

$$\begin{cases} d\sigma_{\rm tot}/d^2b = \langle 2T\rangle\,, \\ d\sigma_{\rm el}/d^2b = \langle T\rangle^2\,, \\ d\sigma_{\rm inel}/d^2b = \left\langle 1 - e^{-\sum 2f_i}\right\rangle\,. \end{cases} \tag{2}$$

If the projectile has an internal structure, the mass eigenstates Ψ_k can differ from the eigenstates of diffraction Φ_n, which have eigenvalues T_n. With the notation $\Psi_k = \sum_n c_{kn}\Phi_n$ (with $\Psi_{\rm in} = \Psi_1$) the elastic amplitude is given by $\langle\Psi_1|T|\Psi_1\rangle = \sum c_{1n}^2 T_n = \langle T\rangle$, while the amplitude for diffractive transition to mass eigenstate Ψ_k is given by $\langle\Psi_k|T|\Psi_1\rangle = \sum_n c_{kn}T_n c_{1n}$. The corresponding cross-sections become

$$d\sigma_{\rm el}/d^2b = \left(\sum c_{1n}^2 T_n\right)^2 = \langle T\rangle^2 \,, \tag{3}$$

$$d\sigma_{\rm diff}/d^2b = \sum_k \langle\Psi_1|T|\Psi_k\rangle\langle\Psi_k|T|\Psi_1\rangle = \left\langle T^2\right\rangle \,. \tag{4}$$

The diffractive cross-section here includes elastic scattering. Subtracting this gives the cross-section for diffractive excitation, which is thus determined by the fluctuations in the scattering process

$$d\sigma_{\rm diff\,ex} = d\sigma_{\rm diff} - d\sigma_{\rm el} = \left(\left\langle T^2\right\rangle - \langle T\rangle^2\right) d^2b \,. \tag{5}$$

3.2. Diffractive eigenstates

In the Lund Dipole Cascade Model [3, 4, 5, 6] it is assumed that a high energy collision is driven by parton–parton subcollisions, in the same spirit as in the model implemented in the PYTHIA MC. At high energies, interactions at small x dominate, where the parton cascade evolution ought to be dominated by BFKL dynamics. Here the gluon density grows very fast, and multiple interactions become important, leading to saturation effects.

A proton cascade is illustrated in Fig. 2. If one of the partons interacts with a target via gluon exchange, (parts of) the cascade can come on shell, and we get an inelastic event. According to the optical theorem this gives a contribution to the elastic scattering, and to diffractive excitation.

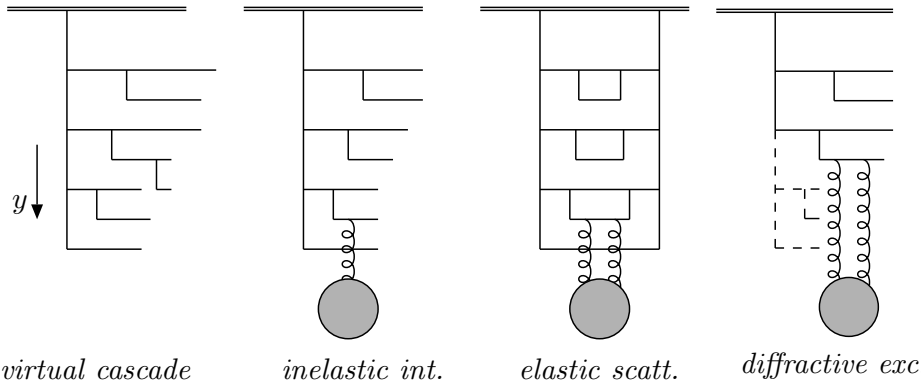


Fig. 2. A parton cascade in a proton can interact with a target via gluon exchange.

3.3. Dipole cascade models

Mueller's dipole cascade model [7,8,9] is a formulation of LL BFKL evolution in transverse coordinate space. Gluon radiation from the colour charge in a parent quark or gluon is screened by the accompanying anticharge in the colour dipole. This suppresses emissions at large transverse separation, which corresponds to the suppression of small $k_\perp$ in BFKL. For a dipole with charges in transverse points $\boldsymbol{x}$ and $\boldsymbol{y}$, the probability per unit rapidity (Y) for emission of a gluon at transverse position $\boldsymbol{z}$ is given by

$$\frac{d\mathcal{P}}{dY} = \frac{\bar{\alpha}}{2\pi} d^2\boldsymbol{z} \frac{(\boldsymbol{x}-\boldsymbol{y})^2}{(\boldsymbol{x}-\boldsymbol{z})^2(\boldsymbol{z}-\boldsymbol{y})^2}\,, \quad \text{with} \quad \bar{\alpha} = \frac{3\alpha_s}{\pi}\,. \tag{6}$$

The dipole is split into two dipoles, which (in the large N_c limit) emit new gluons independently. The result is a cascade, where the number of dipoles grows exponentially with Y.

When two cascades collide, a pair of dipoles with coordinates $(\boldsymbol{x}_i, \boldsymbol{y}_i)$ and $(\boldsymbol{x}_j, \boldsymbol{y}_j)$ can interact via gluon exchange with the probability $2f_{ij}$, where

$$f_{ij} = f(\boldsymbol{x}_i, \boldsymbol{y}_i | \boldsymbol{x}_j, \boldsymbol{y}_j) = \frac{\alpha_s^2}{8}\left[\log\left(\frac{(\boldsymbol{x}_i-\boldsymbol{y}_j)^2(\boldsymbol{y}_i-\boldsymbol{x}_j)^2}{(\boldsymbol{x}_i-\boldsymbol{x}_j)^2(\boldsymbol{y}_i-\boldsymbol{y}_j)^2}\right)\right]^2 . \tag{7}$$

Summing over all dipoles in the cascades then reproduces the LL BFKL result.

The *Lund dipole cascade model* [3,4,5,6] is a generalization of Mueller's model, which also includes:

– NLL BFKL effects,
– Nonlinear effects in the evolution,
– Confinement effects.

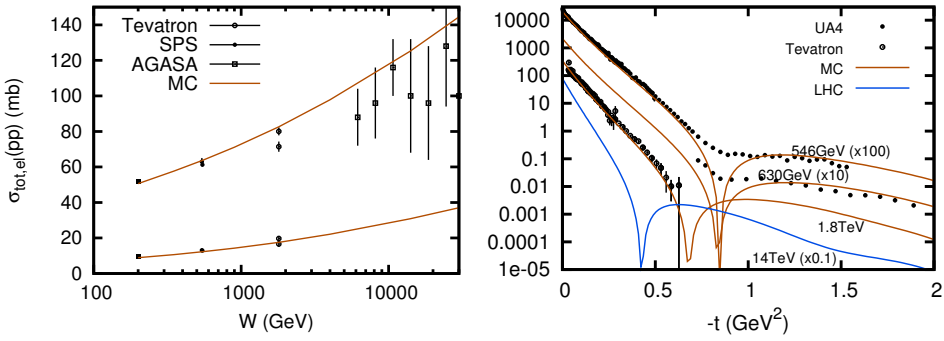


Fig. 3. Total and elastic cross-sections in pp collisions in the dipole cascade model.

For an incoming virtual *photon* splitting into a $q\bar{q}$ pair, the initial state wavefunction is determined by perturbative QCD. For an incoming *proton* we make an ansatz in form of an equilateral triangle of dipoles. After evolution the result is rather insensitive to the exact form of the initial state. The model is also implemented in a MC program DIPSY. The results for the total and elastic cross-sections in pp scattering are shown in Fig. 3. The model also successfully reproduces inclusive and quasielastic cross-sections in DIS [3, 10].

3.4. Diffractive cross-sections

The BFKL evolution gives large fluctuations in the cascade evolution. Let us study the interaction in a frame where the projectile is evolved a distance y_1 and the target $y_2 = Y - y_1$, where Y is the total rapidity range $\approx \ln s/(1\text{GeV}^2)$. If we here first take the average over the target states, we get the amplitude for elastic scattering of the target. Squaring it gives the cross-section, when the target is scattered elastically. If we after this take the average over the projectile states, we obtain the diffractive scattering of the projectile, including the elastic scattering. Thus the expression

$$\left\langle \langle T \rangle^2_{\text{targ}} \right\rangle_{\text{proj}} - \langle T \rangle^2_{\text{targ, proj}} \tag{8}$$

gives the cross-section for single diffractive excitation of the projectile, with the excited mass limited to $M_X^2 < \exp(y_1)$. Varying y_1 gives then $d\sigma/dM_X^2$.

In pp scattering the Born amplitude is large, and therefore the unitarity effects are important. Fig. 4 shows both the Born amplitude and the unitarized amplitude at 2 TeV for different impact parameters b. We see that the width of the Born amplitude is large, and without unitarization the fraction of diffractive excitation would be correspondingly large. (The smooth lines are fits of the form $AF^p e^{-aF}$.)

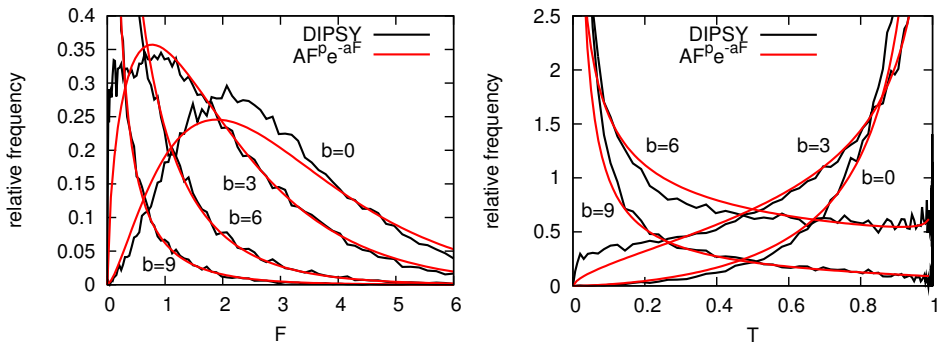


Fig. 4. Distribution in the one-pomeron amplitude F (left), and the uniterized amplitude T (right) in pp collisions at 2 TeV. b is in units of GeV^{-1}.

However, the unitarized amplitude is limited by 1, and the width of the distribution, and therefore the diffractive excitation, is very much reduced. This result corresponds to the effect of enhanced diagrams in the conventional triple-regge approach. The resulting single diffractive cross-section for $M_X < M_X^{(\mathrm{cut})}$ is shown in Fig. 5, together with an estimate from CDF data. We note here also that the strong suppression from saturation implies that factorization is broken when comparing diffraction in pp collisions and DIS.

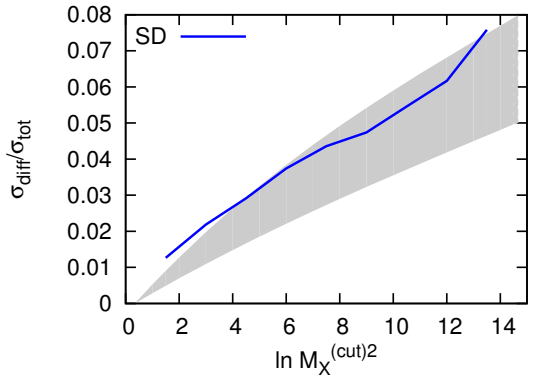


Fig. 5. The single diffractive cross-section for $M_X < M_X^{(\mathrm{cut})}$. The shaded region is an estimate from CDF data [11].

The absorption is most important for central collisions, where diffractive excitation is most strongly suppressed. As shown in Fig. 6 the cross-section for diffractive excitation is therefore largest in a ring with radius $b \sim 1\,\mathrm{fm} \approx 5\,\mathrm{GeV}^{-1}$, which grows slowly with energy. Another consequence of the large saturation in pp collisions, is that factorization is not satisfied when comparing diffractive excitation in DIS and pp scattering.

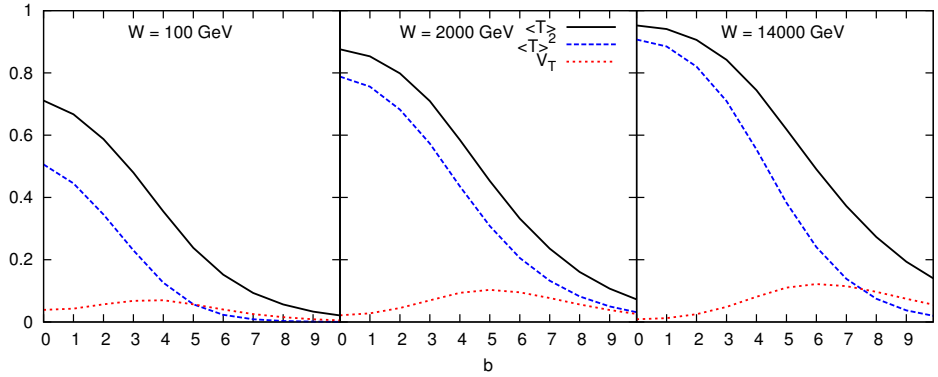


Fig. 6. Impact parameter distributions for $\langle T\rangle = (d\sigma_{\mathrm{tot}}m/d^2b)/2$, $\langle T\rangle^2 = d\sigma_{\mathrm{el}}/d^2b$, and $V_T = d\sigma_{\mathrm{diff\ ex}}/d^2b$ in pp collisions at $W = 2$ TeV. b is in units of GeV^{-1}.

3.5. Comparison with multi-regge analyses

It is also interesting to compare the results from the Good–Walker analysis with the multi-regge formalism. To this end we study the contribution from the *bare pomeron*, meaning the one-pomeron amplitude without contributions from saturation, enhanced diagrams or gap survival form factors.

When s, M_X^2, and s/M_X^2 are all large, pomeron exchange should dominate. If the pomeron is a simple pole, we expect the following expressions for the pp total and diffractive cross-sections

$$\begin{aligned}
\sigma_{\text{tot}} &= \beta^2(0)(s/s_0)^{\alpha(0)-1} = \beta^2(0)(s/s_0)^{\epsilon}\,, \\
\frac{d\sigma_{\text{el}}}{dt} &= \frac{1}{16\pi}\beta^4(t)(s/s_0)^{2(\alpha(t)-1)}\,, \\
M_X^2\frac{d\sigma_{\text{SD}}}{dtd(M_X^2)} &= \frac{1}{16\pi}\beta^2(t)\beta(0)g_{3P}(t)\left(\frac{s}{M_X^2}\right)^{2(\alpha(t)-1)}\left(M_X^2\right)^{\epsilon}\,. \qquad (9)
\end{aligned}$$

Here $\alpha(t) = 1 + \epsilon + \alpha' t$ is the pomeron trajectory, and $\beta(t)$ and $g_{3P}(t)$ are the proton–pomeron and triple-pomeron couplings respectively. Comparing our result with this expression, we find that it indeed reproduces the triple pomeron form, with the following parameter values obtained choosing the value $s_0 = 1$ GeV^2 for the arbitrary scale parameter [5]

$$\begin{aligned}
\alpha(0) &= 1 + \epsilon = 1.21\,, \qquad \alpha' = 0.2\ \text{GeV}^{-2}\,, \\
\beta^2(0) &= 12.6\ \text{mb}\,, \qquad \beta(t) = \beta(0)\exp\left(\frac{2.5\,t}{1-1.8\,t}\right)\,, \\
g_{3P}(t) &= \text{const.} = 0.3\ \text{GeV}^{-1}\,. \qquad (10)
\end{aligned}$$

4. Nucleus collisions (preliminary results)

Our model can also be applied to nucleus collisions, where it gives a full partonic picture, including fluctuations. As an example, Fig. 7 shows the dipole distribution in a peripheral Au–Au collision at RHIC. A possible application would be to use the corresponding energy and momentum densities as initial state for a hydrodynamic expansion. The resulting hadron distribution could then also be compared with the result obtained from ordinary string hadronization, assuming no plasma formation.

Another application is obtained from studies of triangular flow, v_3. Although v_3 must vanish by symmetry for averaged distributions, fluctuations can give nonzero results, and it has recently been suggested that triangular flow can be the origin for what has been interpreted as a Mach cone or Cherenkov radiation, see *e.g.* [12]. As an example, Fig. 8 shows the transverse energy density in peripheral Pb–Pb collisions at LHC. The left

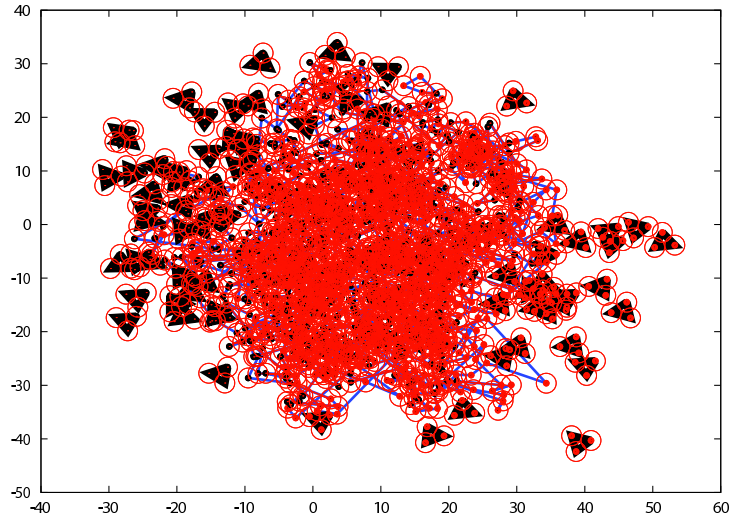


Fig. 7. Dipole distribution in a peripheral Au–Au collision at RHIC.

figure shows the distribution in a single individual event. For comparison the right figure shows the distribution averaged over many events. We see that although the average distribution is symmetric, the individual event has a clear asymmetry, leading to a nonzero value for v_3[1].

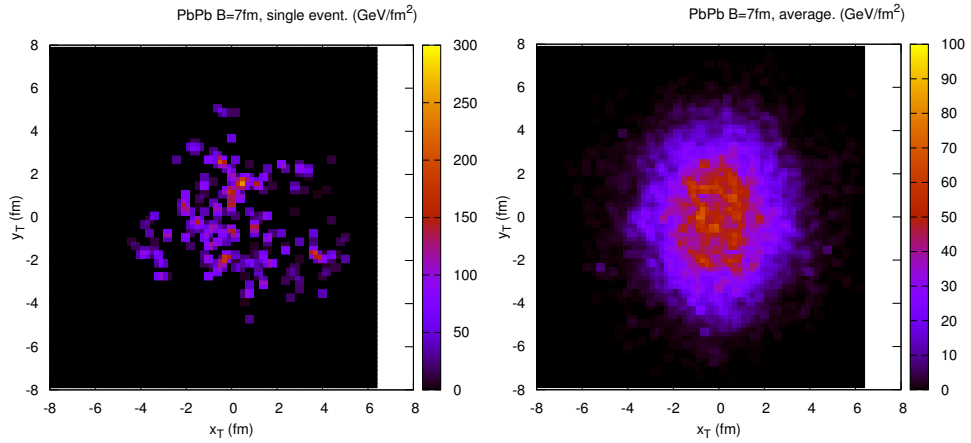


Fig. 8. $E_\perp$ density in Pb–Pb at LHC and $b = 7$ fm. Left: A single event. Right: Average over many events. Note the different colouring in the two figures.

[1] A more detailed study [13] has been published after the presentation of this talk.

5. Summary

- Fluctuations have important dynamical effects.
- Andrzej often has pointed out new phenomena.
- In Lund we also try our best.

Congratulations on the 75th birthday!

REFERENCES

[1] G. Gustafson, A. Nilsson, *Nucl. Phys.* **B355**, 106 (1991).
[2] B. Andersson, P. Dahlqvist, G. Gustafson, *Z. Phys.* **C44**, 455 (1989).
[3] E. Avsar, G. Gustafson, L. Lönnblad, *J. High Energy Phys.* **0701**, 012 (2007) [arXiv:hep-ph/0610157v2].
[4] E. Avsar, G. Gustafson, L. Lönnblad, *J. High Energy Phys.* **0712**, 012 (2007) [arXiv:0709.1368v3 [hep-ph]].
[5] C. Flensburg, G. Gustafson, *J. High Energy Phys.* **1010**, 014 (2010) [arXiv:1004.5502 [hep-ph]].
[6] C. Flensburg, G. Gustafson, L. Lönnblad, *J. High Energy Phys.* **1108**, 103 (2011) [arXiv:1103.4321v2 [hep-ph]].
[7] A.H. Mueller, *Nucl. Phys.* **B415**, 373 (1994).
[8] A.H. Mueller, B. Patel, *Nucl. Phys.* **B425**, 471 (1994) [arXiv:hep-ph/9403256v2].
[9] A.H. Mueller, *Nucl. Phys.* **B437**, 107 (1995) [arXiv:hep-ph/9408245v1].
[10] C. Flensburg, G. Gustafson, L. Lönnblad, *Eur. Phys. J.* **C60**, 233 (2009) [arXiv:0807.0325 [hep-ph]].
[11] F. Abe *et al.* [CDF Collaboration], *Phys. Rev.* **D50**, 5535 (1994); *Phys. Rev.* **D50**, 5550 (1994).
[12] B. Alver *et al.* [PHOBOS Collaboration], *Phys. Rev.* **C81**, 034915 (2010) [arXiv:1002.0534 [nucl-ex]].
[13] C. Flensburg, arXiv:1108.4862v1 [nucl-th].